

Active bending in plywood floor structures with in-plane curvature

Flexión activa en forjados contrachapados con curvatura en el plano

Alfonso García Santarbarbara^(*), Juan Monjo Carrió^(*), Hiroyasu Sakata^(**), Ramón Sastre Sastre^(***)

ABSTRACT

Active bending structures incorporate curved beams or shells that are elastically bent from originally straight or flat elements. When both curved and straight elements are coupled, systems stiffness can be enhanced for certain load cases. In this paper, the effects of active bending in twelve floor structure proposals constructed from curved and straight plywood elements is discussed. These solutions are numerically analysed and compared with the reference solution of straight and parallel joists in a Bic- λ diagram, the instrument devised by Frei Otto to compare the material consumption of different structural systems. Simultaneously to the analytical study, three-point bending tests of two full-scale prototypes are carried out. Based on tests findings, a new case of joist with more elements is introduced, which will eventually be the most efficient.

Keywords: active bending; lauan; plywood; floor frame; structural efficiency; Bic-lambda.

RESUMEN

Las estructuras con flexión activa incorporan vigas o superficies curvas que obtienen esa geometría mediante deformación elástica de elementos originalmente rectos o planos. Cuando se emparejan elementos curvos y rectos se pueden conseguir sistemas con una rigidez mayor que si trabajan independientemente. En este trabajo se estudian los efectos de la flexión activa en doce propuestas de forjado con viguetas construidas a partir de elementos curvos y rectos de contrachapado de lauan. Estas soluciones se analizan informáticamente y se comparan con la solución de referencia de viguetas rectas y paralelas en un diagrama *Bic- λ* , el instrumento ideado por Frei Otto para comparar el consumo material de distintos sistemas estructurales. Simultáneamente al estudio analítico se realizan ensayos a flexión de tres puntos de dos prototipos a escala real. Las conclusiones derivadas de los ensayos servirán para introducir un nuevo caso de vigueta con más elementos que acabará siendo el más eficiente.

Palabras clave: flexión activa; lauan; contrachapado; forjado; consumo estructural; Bic-lambda.

(*) Higher Technical School of Architecture of Madrid UPM, Madrid (Spain).

(**) Tokyo Institute of Technology, Tokyo (Japan).

(***) Higher Technical School of Architecture of Vallès UPC, Sant Cugat del Vallès (Spain).

Persona de contacto/Corresponding author: alfonsogarsan@gmail.com (A. García Santarbarbara)

ORCID: <https://orcid.org/0000-0001-9176-0950> (A. García Santarbarbara); <https://orcid.org/0000-0003-2191-834X> (J. Monjo Carrió); <https://orcid.org/0000-0002-2388-8626> (R. Sastre Sastre); <https://orcid.org/0000-0002-6648-4015> (H. Sakata)

Cómo citar este artículo/Citation: García Santarbarbara, Alfonso; Monjo Carrió, Juan; Sakata, Hiroyasu; Sastre Sastre, Ramón (2022). Active bending in plywood floor structures with in-plane curvature. *Informes de la Construcción*, 74(568): e473. <https://doi.org/10.3989/ic.91082>

Copyright: © 2022 CSIC. This is an open-access article distributed under the terms of the Creative Commons Attribution 4.0 International (CC BY 4.0) License.

Recibido/Received: 23/09/2021

Aceptado/Accepted: 09/04/2022

Publicado on-line/Published on-line: 17/11/2022

1. INTRODUCTION

1.1. Active bending

The term *active bending* was first introduced in 2010 by several German authors -Lienhard, Schleicher, Knippers, Alpermann and Gengnagel- (1, 2) to designate those structures with curved elements, beams or plates, which base their geometry on the elastic deformation of originally linear or flat elements. Although the term was coined in this century, it refers to a very old practice. Since the emergence of the first civilizations, there have been examples of construction solutions that incorporate the elastic behavior of building materials. When the designer of structures chooses to introduce elastic bending into the construction process, some kind of benefit is expected: the development of an efficient and transportable structural system in the case of the Mongolian yurt or the Madan mudhif (from approx. 3000 B.C.) (3), simplifying the construction process as in Armand-Rose Émy's barracks in Marac (1825) (4), the achievement of an optimal form in the case of the Mannheim multihalle designed by Frei Otto (1975) (5) (figure 1), or some stiffness enhancement as the ICD/ITKE 2010 pavilion (1).

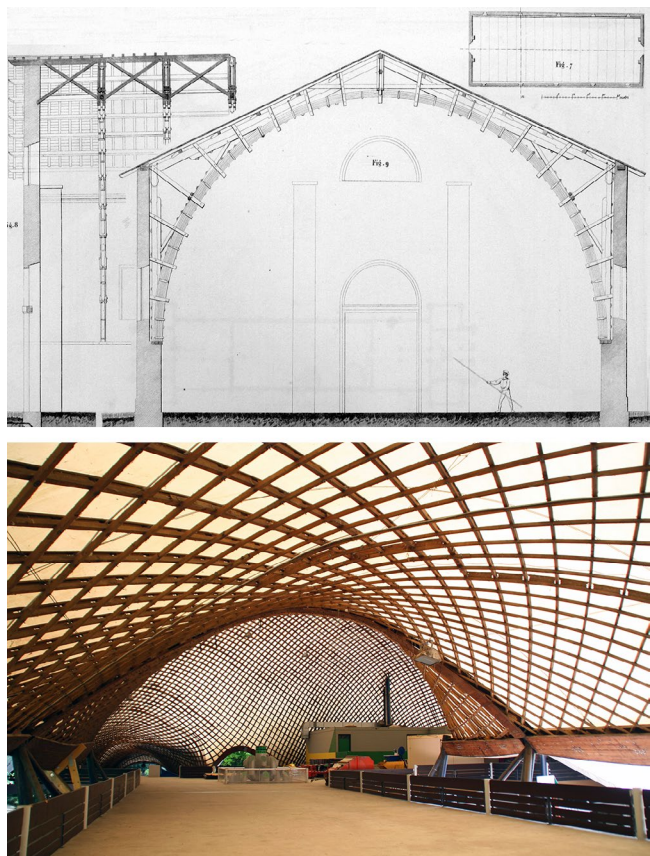


Figure 1. Top: Armand-Rose Émy's barracks in Marac (1825). Source: (4), plate 102. Bottom: Mannheim multihalle.

Most of the practical examples that use active bending employ this technic to build roofs or lateral envelopes. However, a lack of proposals has been identified that have considered its use to lighten a wooden floor frame. This lack represents an area of opportunity to research, which would also solve the fact that the design criterion for lightweight wooden floor frame is not strength or stability, but rather, in most situations, stiffness. The remaining strength that is not exploited

can be used in a form-finding process, if this leads to enhance the overall stiffness of the solution.

This research focuses on the analysis of a group of lightweight wooden floor frame proposals constructed only with plywood and where some elements are bent by means of cold elastic deformation. It aims to find solutions more efficient than the usual ones made from straight beams. In order to objectively quantify the benefit, the concept of quantification of structural consumption devised by Otto, *Bic*, (6) is calculated for each proposal. Since the term *Bic* was coined in 1954, it has been used for the evaluation of lightweight constructions (7, 8) and even of natural structures such as plant stems (9, 10). García Santabárbara and Cervera Bravo, 2017, (11) presented this concept and applied it to a single active bending structure. In the present study, the use of the *Bic*- λ diagram is proposed to compare different active bending solutions with respect to the system built of straight and parallel joists, and eventually obtain the most efficient scheme of the group.

1.2. Quantification of structural consumption. Modified *Bic*- λ diagram

The working group of the IL (Institute for Lightweight Construction at the University of Stuttgart), led by Frei Otto, developed and explained thoroughly in (6) a practical tool for evaluating the efficiency of any structure and comparing it with others: the *Bic*- λ diagram (figure 2).

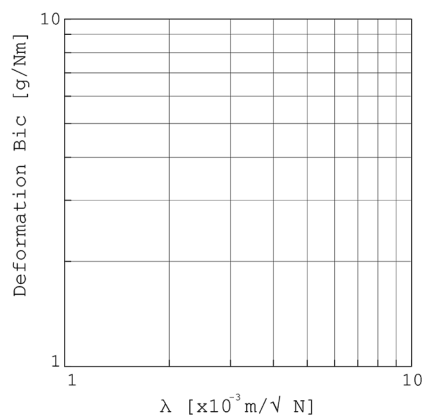


Figure 2. *Bic*- λ diagram. Elaborated from Otto et al., 1998.

For Otto, the term lightweight expresses, in the field of mechanics of materials, the relationship between the mass of an object and its capacity to transmit loads. In fact, he invented a secondary physical quantity to measure the lightness of any object, *Bic*, shown on the ordinate axis of the diagram. The concept *Bic* represents, therefore, the inverse of the efficiency of the mass used to solve the transmission of forces –or *Tra*– that the structural problem poses. That is, the lower the *Bic* of an object is, the higher its efficiency stands.

$$[1] \quad Bic = m/T$$

where m represents the mass of the solution, and T is the symbol of the physical quantity called *Tra*. When a structure is loaded, *Tra* can be determined by equation [2] from the transmitted forces, F , and the transmission distance of each force, s .

$$[2] \quad T = \Sigma F \cdot s$$

Normally, when Otto uses the term *Bic*, he refers to the ultimate-load *Bic*, determined by the load that produces a total or partial collapse of the system. However, he defines other types of *Bic*, such as the material *Bic*, which is calculated by dividing density by ultimate stress, or those due to live, dead, traffic or even energy loads. Among the different options, the most interesting for a research on structures with large displacements and/or governed by the stiffness criterion, is the deformation *Bic*. The *Bic* values included in this work are those measured for loads that make net final deflection from Eurocode 5 to be lower than 1/300. So, in the proposed modified diagram, the ordinate axis represents deformation *Bic* instead of ultimate-load *Bic*.

For Otto, *Tra* concept is independent of the direction and sense of forces. Destabilizing effects of compression or bending must be incorporated by another quantity, λ , which is placed on the abscissa axis of the diagram. This new concept relates form and sense of forces, and is called by Otto relative structural slenderness. This name shows the connection to formal slenderness (s/b which means length divided by cross-section width).

$$[3] \quad \lambda = s/\sqrt{F}$$

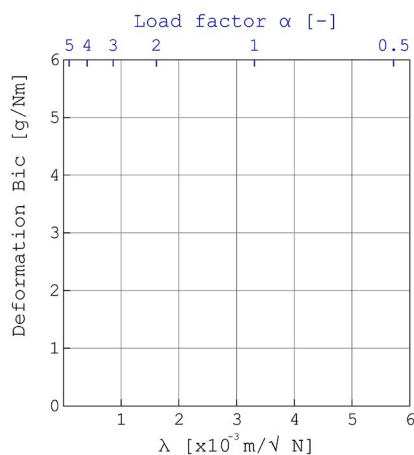


Figure 3. Adapted Bic- λ diagram.

All the proposals developed in this study have the same scheme – pinned horizontal flat surfaces with downwards uniformly distributed load -, so the load path, s , is kept constant. Then, the slenderness λ axis also represents the load. A second auxiliary abscissa axis is introduced at the top of the adapted diagram, with the values of the load factor with respect to the quasi-permanent combination defined by Eurocodes. Last adaptation from Frei Otto’s diagram is to use decimal scale in order to improve its readability (figure 3).

2. MATERIAL AND METHODS

This research is supported by a combination of theoretical principles, virtual models and physical experiments. The research methodology follows the workflow of most of the active bending structure projects, where generally theory is validated by digital simulation and finally tested by building a prototype (12, 13).

All the studied proposals are built entirely with *lauan* plywood, nails and screws. Materials characteristics and properties are shown in section 2.1, while design motivation and construction aspects are explained in section 2.2. Mass reduction is evaluated by comparison with a system of straight and parallel joists, which geometrical parameters are described in section 2.3. Once constructions conditions are established, numerical analyses are done by means of computer simulation (details in section 2.4). Two full-scale prototypes are built and loaded to check digital protocol and prestress impact. Test conditions are defined in section 2.5. Results of both analytical and experimental stages are presented in section 3.1 and 3.2, respectively. Finally, process conclusions are drawn in section 4.

2.1. Material properties

The only wooden material used in the group of floor frame proposals is *lauan* plywood. According to the Wood Handbook from U.S. Forest Products Laboratory (14), *lauan* is the common market name applied to four groups of Southeast Asian species of *Shorea*. Other common names for *Shorea* species are *meranti* or *Philippine mahogany*. These *lauan-meranti* groups are divided depending on heartwood color and density. The plywood used in the construction of the full-scale models was characterized by weight and visual inspection. The result of these tests showed that mockups were built with light red *lauan*. Tropix 7 (15), the french public funding catalog of technical data sheets for tropical and temperate forest species, lists the two most commonly traded species under the light red *lauan-meranti* group: *Shorea parvifolia* and *Shorea macroptera*.

The commercial group of *lauan-meranti* species makes up a large percentage of the total hardwood plywood imported into the United States and Japan. Actually, *lauan* is by far the most common wood species used in JAS-compliant type 1 plywood (16). JAS means Japanese Agricultural Standard, and is the Japanese standard that defines the properties of plywood to be qualified for structural use-. JAS-compliant type 1 is the best plywood to build active bending structures as it has the smallest minimum radius of curvature (106 times the material thickness, 12 mm), while birch or pine plywood have bigger radius (125 and 178 times the thickness, respectively).

JAS standard sets minimum thresholds for strength and stiffness, and allows the manufacturer to choose the panel composition. This causes the actual strength and stiffness of the panels to be higher than that defined by the standard. So tensile, compression and flexural tests were carried out to characterize the properties of 12 mm *lauan* plywood. Plies thickness of tested 12 mm plywood is 1.5+3+3+3+1.5 mm. Table 1 shows the values of main bending material properties referred to with Eurocodes notation. JAS values are used in FEM models made for general comparisons. When the computerized model is built to contrast to prototypes, then the values resulting from especific characterization tests are employed.

Where $f_{m,o,k}$ is characteristic bending strength of the panel working as a board, $E_{o,mean}$ is the mean value of modulus of elasticity of the panel working as a board and $f_{y,o}$ is yield strength. The letter “o” in the subindex specifies that the property is measured along the grain of the two outer plies.

Table 1. Plywood properties along the grain [N/mm²].

Material	JAS		Material characterization test		
	$f_{m,o,k}$	$E_{o,mean}$	$f_{m,o,k}$	$f_{y,o}$	$E_{o,mean}$
9 mm plywood	28.00	6500	No tests needed		
12 mm plywood	24.00	5500	35.80	18.62	8586
18 mm plywood	22.00	5000	No tests needed		

Horizontal panels are nailed to vertical ones with 1 mm diameter and 25 mm long nails each 75 mm. These pin dimensions prevent the plywood from splitting when nailing to the edge of the panel. 18 mm finishing panel is screwed to top sheathing by 3.5 diameter and 32 mm screws. Screws are arranged following a rectangular array which spacing is 75x400 mm. Main mechanical properties for these connectors are detailed in table 2, where $F_{v,Rk}$ is characteristic load-carrying capacity per shear plane per fastener and K_{ser} is the slip modulus.

Table 2. Connectors properties.

Material	$F_{v,Rk}$ [N]	K_{ser} [N/mm]
1x25 mm nail	184	478
3.5x32 mm screw	825	1301

2.2. Plywood floor frame proposals with in-plane bending

The family of case studies with in-plane bending examines solutions composed of horizontal panels that remain flat and vertical elements that can be bent. The curved elastica can be consolidated by grouping the vertical elements and incorporating straight components. From a general point of view, bent vertical elements increase stability against lateral deformations due to curved shape and because of loading paths inside the member. Moreover, straight vertical elements can benefit from the effects of prestressing. All the family cases have the same length -3000 mm- and the same depth -228 mm-.

The first case study, case CP1, is intended to facilitate the on-site construction and assembly process (figure 4). It consists of vertical panels with staggered connections to adjoining panels. The carpenter connects each panel by four bolts to the next and previous ones. Joint distance is approximately one-third and two-thirds of its length, respectively. This operation is repeated until the set of joists covers the full width of the slab section. When it arrives on site, it can be quickly unfolded by introducing some blocks at both ends. The sinusoidal elastica that appears is determined only by the length of the panels and the final spacing of the ends, so horizontal panels can be marked with nailing reference lines. The end result is a surface element that can be lifted into its final position fully assembled, reducing occupational hazards as it can be used immediately as the next working surface.

In the following cases, the option of coupled systems is explored, so independent joists are built and nailed later to the horizontal panels. These joists are composed of an odd

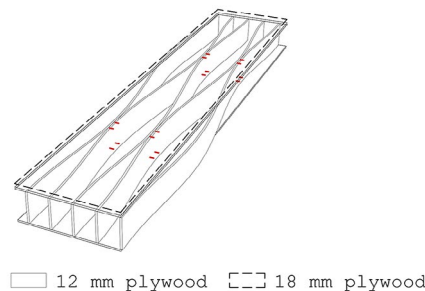


Figure 4. Case CP1.

number of initially flat vertical panels arranged symmetrically. The central component is slightly shorter than the two adjoining ones, and these are slightly shorter than the outer ones. When both ends of the panels are brought together and anchored, the central one is stretched while the rest are compressed and bent. The CP2 joist consists of three elements (two bent and one straight component), the CP3 proposal consists of five (four bent and one straight component) and the CP4 solution adds to the three-element joist a fourth one equidistant exterior straight component.

The design criterion for timber floor frames is generally the deflection for the appearance requirement. Compliance with this requirement can be achieved by introducing camber in the opposite direction to that caused by the service load. Execution camber is usually achieved with the shape of the piece, but here two methods for introducing camber by exploiting active bending have been considered. The first approach, used in case CP2a (figure 5), is based on arranging the bolts at the ends of the three vertical panels asymmetrically with respect to the longitudinal axis. If they are located at the top, the upper fibers of the straight elements have greater tension than the lower ones and the vertical elements deform with the convex part upwards. Within the second method, called case CP2b, bolts are distributed in a symmetrical arrangement. In order to ensure that the upper fibers of the straight element have higher stress, the lower part of the curved panels is cut off in the vicinity of the support. Thus the stresses are concentrated on the bolts at the top, producing an eccentricity that generates support rotation.

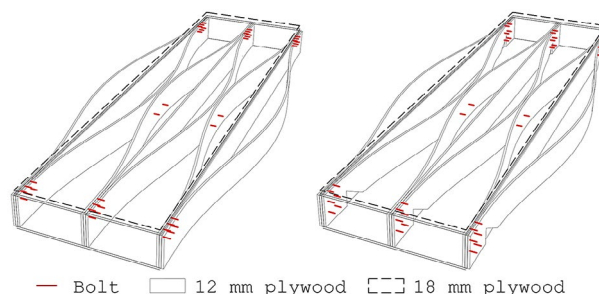


Figure 5. Case CP2a –left- and CP2b –right-.

If the elastica of the bent elements is maintained, i.e. the radius of curvature for each point, choosing a thinner panel means to reduce the forming stress, according to Euler-Bernoulli law. But it also reduces the tensile stress of the straight element. Derived from three-point bending test results (see conclusions) and following the Latin phrase “*Divide et impera*”, it is proposed to distribute the material in more bent

elements. The symmetry conditions with respect to the central panel must be maintained, so it does not buckle. In the case of CP3a (figure 6), the added elements have half the depth, since the intention is to evaluate their influence on the induced tensile stress, and consequently on the camber. When all the elements have the same depth, as in case CP3b, tie thrust is increased, but in addition to this, the new vertical panels are connected to the lower horizontal one.

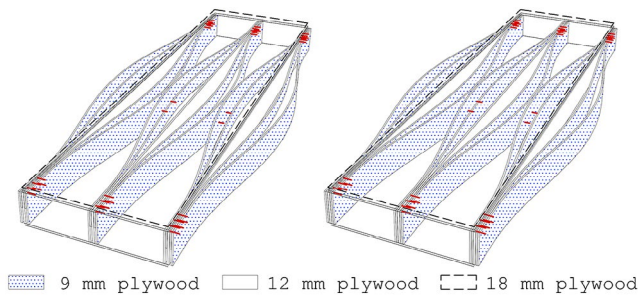


Figure 6. Case CP3a –left- and CP3b –right-.

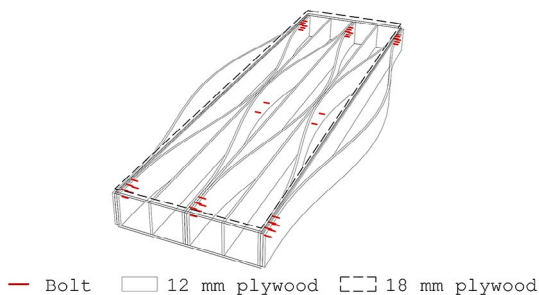


Figure 7. Case CP4.

The rolling shear strength set by the JAS standard for structural panels (Class 1) is relatively low. Concentrated load hypothesis especially affects to shear calculations. All the proposals include an 18 mm plywood finishing layer screwed to the 12 mm upper sheathing in order to withstand the increment of shear stress for concentrated load. Since the shear value at the support mainly depends on the span, solution CP4 (figure 7) proposes to reduce the joist spacing in the area close to the support by including an intermediate straight vertical panel.

Two system versions are distinguished for each case: those designated as *_1t*, which only have an upper horizontal sheathing; and those marked as *_2t*, which are solved with two horizontal sheathings both at the top and at the bottom. The static behavior is different, but there are also differences in their behavior in case of fire. In the proposals without bottom protection, the vertical elements have three faces exposed to fire and require a larger cross-section. However, the versions with two sheathings have only one exposed face and considerably increase their fire resistance time. This fact allows the choice of vertical elements with a smaller thickness, which facilitates their bending.

2.3. Straight and parallel joists system

The concepts “*straight joists system*” or “*straight and parallel joists system*” will be referred to intermittently throughout this document. Both expressions are intended to designate

the same construction system. In the context of this paper, straight joists system is the one that solves the structural problem only with straight and flat elements, i.e. without including active bending. Straight and parallel joists system is instrumentalized as a reference for mass comparison. Every active bending solution will be referred to the corresponding straight joists system that reaches the same deformation under the same load and with the same depth. The masses of both systems with the same global stiffness will then be compared. Since the thickness of the panels is limited to the off-the-shelf values, joists spacing is parameterized to find the corresponding straight joists system with the same stiffness. Figure 8 shows two of the different values for joist spacing and at the same time both system configuration with one and two sheathings. In this way, a continuous curve is obtained in the *Bic-λ* diagram, and all the solutions with active bending have one reference to establish the mass variation. Straight and parallel joists system is made entirely of the same material as the rest of the proposals: *lauan* plywood.

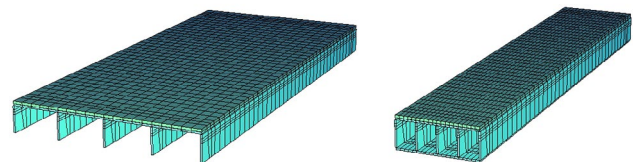


Figure 8. Examples of different joists spacing for both configurations of straight joists system. Left: Configuration without bottom sheathing and 3 joists per linear metre. Right: Configuration with bottom sheathing and 7 joists per linear metre.

2.4. Analytical study methodology: FEM simulation

Bathe, 1996 (17) defines three modes of nonlinearity: material, geometric and the mixture of the two previous. If yield point is reached, stress-strain ratio is no longer linear and material nonlinearity appears. When the structure is loaded and geometry changes are non neglectable, it is called geometric nonlinearity. Then elastica must be considered as an intermediate geometry in the calculation and an iterative process is needed.

During the elastic bending procedure, large displacements and large rotations arise, so active bending structures are affected by geometric nonlinearity. Nevertheless, strain is usually small, so no yielding is taken into account, and stress-strain law is maintained linear.

All the structural systems presented here are simulated by Finite Element Modelling run in the commercial software package Sofistik. This software makes difference between second and third order theory analysis. Second order calculation computes π -delta effect, but third order also takes rotation into account in the deformation process. As load-deflection ratio is no linear, stiffness matrix is no constant and equilibrium path must be divided in successive load steps which are computed by several iterations. Updating the stiffness matrix is the main cause to increase computing time. Sofistik employs Modified Newton-Raphson method where tangential stiffness matrix is assembled only before every load step. Just in the case that convergence is not reached, stiffness matrix is exceptionally updated within load step, after the iteration where divergence occurs.

2.5. Bending test methodology

At an intermediate point of the research, a full-size prototype test was considered. This test was approached as an experiment to observe the real effects of active bending, so it was focused on trying to isolate bending results, and not on the verification of a definitive proposal. In this sense, a test protocol was developed for *CP2a_1t* proposal, the one with the three-element joist and without bottom sheathing, in order to reduce the number of components as much as possible and to minimize any events that could affect the bending process. Totally, two specimens were tested, one specimen for *CP2a_1t* proposal with top sheathing, and one auxiliary specimen without it.

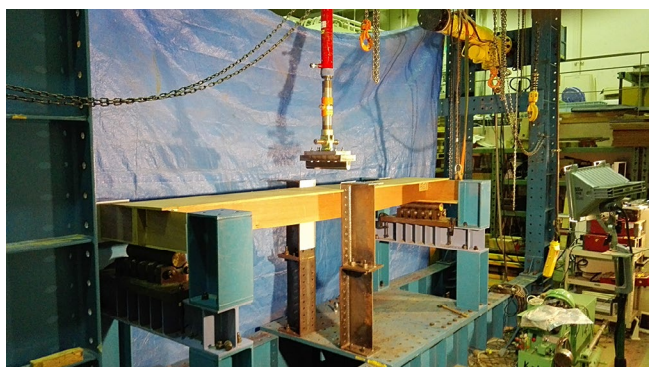


Figure 9. Bespoke three-point bending test setup for large scale structural testing frame.

Specimen dimensions (a full-scale mockup of a construction system) did not allow the three-point bending test to be carried out on a universal or Amsler type machine, and it was necessary to adapt the configuration of the experiment to be carried out on a large scale structural testing frame (figure 9).

The actuator used for load application is a manually operated hydraulic jack. A compression load cell was installed between actuator and mockup. Load cell model is CLP-200KNB from *Tokyo Sokki Kenkyujo*, with a capacity of 200 kN and an accuracy of 0.1 kN. Loading head, bespoke, has a diameter of 40 mm and a length equal to 390 mm. Supports distance is 2800 mm and are made of 80 mm diameter steel cylinders. In order to reduce yielding because of perpendicular-to-grain compression by support cylinders, steel plates with dimensions 320x140*6 mm were introduced. The average speed for the three-points bending test was 0.11 mm/s, which means an approximate test duration of 360 s.

3. RESULTS AND DISCUSSION

3.1. Comparison between cases by means of computer simulation

The global depth of all the proposals presented is identical, 228 mm, regardless of whether the scheme has one or two sheathings. This value is constant at every point, as both surfaces run parallel. In sum, all of the proposals occupy the same space and none of them is better from a volumetric point of view.

Concerning construction process, no case is clearly better than any other. All of them can be transported with the elements already cut in their flat format and be built “in situ”

with the help of auxiliary clamps and sockets that are later removed for reuse. This construction methodology would facilitate their distribution to sites with difficult access. However, as all the solutions have a constant depth, in general terms, it is most practical for all of them to be assembled in the workshop and transported as slabs to be finished on site. If cross-section is not modified throughout panel length, found form is independent of material and elastica depends only on length ratio. Cutting, forming, assembly and nailing can be easily programmed, and manufacturing process could be performed entirely by 6-axis robot at workshop. All the active bending proposals could be standardized and mass produced by a robot-assisted manufacturer.

In order to incorporate the fire response in the evaluations, each active bending case is compared with its respective conventional reference system, in its version with 1 or 2 sheathing layers. So, if the active bending scheme includes bottom sheathing, it is compared with the corresponding straight joists solution that also has it, since this serves as protection in case of fire. The fire resistance of the proposals with bottom sheathing is ostensibly better than those without, since only one face is exposed to fire.

Figure 10 shows the diagram *Bic-λ* of all the proposals that incorporate active bending and straight and parallel joists system. Since *Bic* concept is the inverse of the efficiency, a proposal that is found in the lower part of the diagram is more efficient than another placed in the upper part. The stiffness of a design can be read by means of the secondary abscissa axis at the top of the diagram, which determine the load that produces limit net final deflection. In this sense, straight joists system without bottom sheathing (continuous line) is less stiff but more efficient than the same solution with two sheathings (dashed line). The increase in efficiency can be explained by the fact that the connection between vertical and horizontal panels is far from behaving as an extruded section, and bending moment is being supported mainly by the vertical panels. All the active bending cases studied increase their stiffness through the introduction of the bottom sheathing. However, contrary to the straight joists systems, all the schemes with in-plane bending, except the *CP1* case, manage to improve their efficiency in their version with two sheathings (figure 5).

The comparison of each active bending proposal with the straight joists system with the same deformation for the same load case is summarized in Table 3. This table helps to read figure 10 by means of percentage. The most relevant differences appear for the version with two sheathings. It can be appreciated that *CP1* case is not able to reduce mass with respect to straight joists system so manufacturing effort is not worth it. *CP4* solution with two sheathings reduces material consumption, but not significantly. Its use would be restricted to the situations when concentrated load effects are relevant. If load values and geometry are maintained, finishing panel thickness cannot be reduced, so this solution is discarded. Nevertheless, mass reduction of *CP2* and *CP3* solutions, 8.40 and 11.07% respectively, justifies a more detailed analysis.

In the five-element joist proposal *CP3a*, the new intermediate bent elements serve to increase the camber. The increase is so relevant, that this is the scheme with the largest camber (table 4). However, this value does not even reach 25 % of the usual

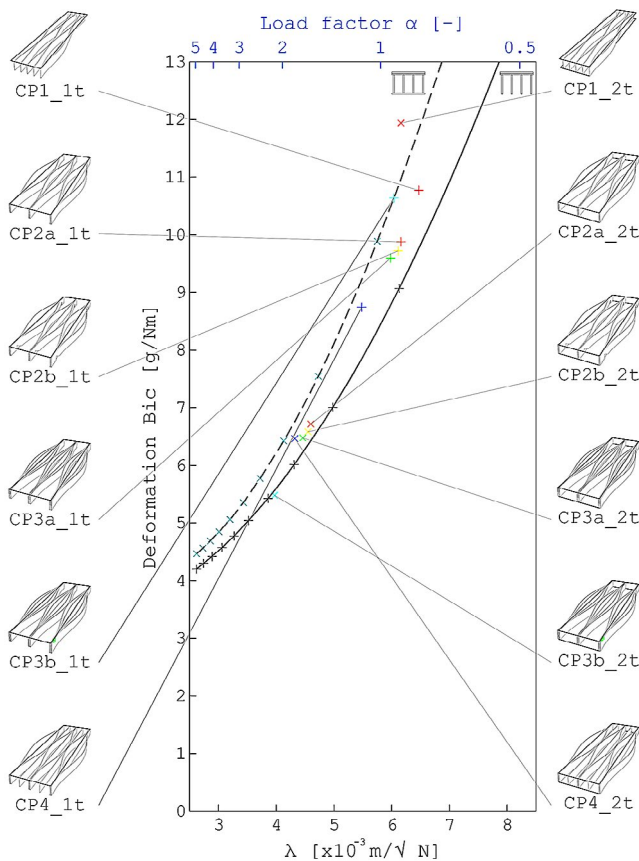


Figure 10. Bic- λ diagram of the family of proposals with in-plane bending.

Table 3. Mass variation with respect to straight and parallel joists system. *_1t* is one sheathing solution and *_2t* has two sheathings.

Case name	<i>_1t</i> version	<i>_2t</i> version
CP1	+10.30%	+8.88%
CP2a	+8.17%	-7.79%
CP2b	+7.63%	-8.40%
CP3a	+9.33%	-7.67%
CP3b	+19.63%	-11.07%
CP4	+11.43%	-4.32%

camber, set as 1.35 – 1.45 times instantaneous deflection for permanent loads. As the new curved intermediate elements depth is half of the others, they are not connected to bottom sheathing, and their torsional strength depends only on the lever arm between the end bolts, so final deflection is minimally reduced compared to the value of *CP2a*, with three elements.

Table 4. Camber, net final and final deflection.

Case name	Camber [mm]	Net final deflection [mm]	Final deflection [mm]
CP1_2t	0.000	10.499	10.499
CP2a_2t	-0.128	5.790	5.918
CP2b_2t	-0.408	5.564	5.972
CP3a_2t	-0.552	5.271	5.823
CP3b_2t	-0.501	4.089	4.590
CP4_2t	-0.128	5.088	5.216

Nevertheless, when the intermediate curved panels are connected to the lower sheathing, case *CP3b_2t*, the scheme improves qualitatively and the most efficient proposal is achieved. Actually, it is the only active bending proposal that manages to be below the curve of the straight and parallel joists solution with only top sheathing (figure 10).

If cases from *CP2* and *CP3* groups are compared, it is observed that the proposals with the largest amount of material that is not connected with the lower sheathing (cases *CP3b_1t* and *CP3a_2t* for the versions with 1 and 2 sheathing, respectively) are the least efficient. Therefore, efficiency improvement has to do with a better performance of the connection between the vertical panels and the lower sheathing.

Figure 11 shows the distribution of normal stress in midpoint cross-section of system with straight joists system spaced 100 mm (left) and *CP3b_2t* solution (right). The spacing between vertical elements of straight joists system is that which equals the unitary weight of timber of the five-element joist proposal, with a consumption of 37.95 kg of timber per square metre of floor. The blue hatch shows stress due exclusively to quasi-permanent load combination. In order to isolate the effects due to external loading, stress values for the straight elements of active bending solutions have been obtained by accepting the application of superposition principle and subtracting residual stress obtained during form-finding process. The red dashed line shows the final values that do include residual stress.

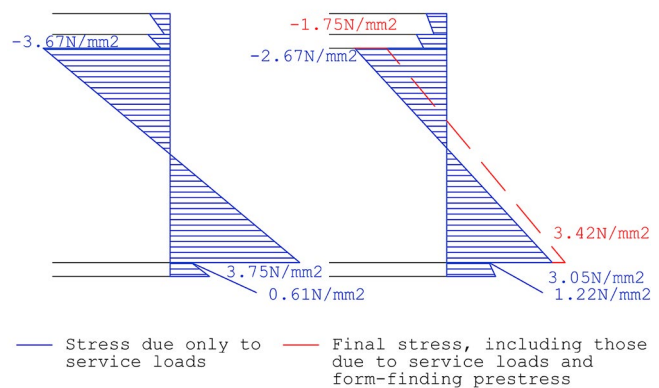


Figure 11. Normal stress distribution for the straight panels of: straight joists system with vertical panels spaced 100 mm (left) and *CP3b_2t* solution (right).

The average stress of finishing panel, top sheathing and bottom sheathing of *CP3b_2t* proposal are, respectively, 28 %, 70 % and 50 % higher than those of straight joists solution. This better exploitation of the horizontal panels leads to a reduction in the stress of the vertical ones. As these vertical panels are all made of the same material, 12 mm thick plywood, the reduction of stress means a smaller strain, a larger radius of curvature and consequently a smaller deflection.

CP3 proposals are less efficient than *CP2* if no bottom sheathing is installed (table 3). This fact can be explained by analyzing the mode of deformation (figure 12). In the form-finding process of the joists, the outer panels are bent laterally, and their upper part, where the bolts are located, is slightly more separated from the straight element than the lower part

(1 mm difference between the upper and lower part). If finishing and top sheathings are nailed and evenly loaded, the curved panels of an isolated joist twist, and the upper part of the midpoint moves further away, while the lower part moves closer to the tie element. When the five-element joist is installed within a complete floor system without bottom sheathing, the upper part of the outer curved elements rests on the upper part of their analogues of the adjacent joist and prevent twisting. However, the intermediate curved panels do not have this lateral support, and lacking the movement restriction provided by the bottom sheathing, their lower part in the midpoint area moves inwards by 16 % of the form-finding lateral displacement. In summary, the intermediate curved panel, if it is not connected to the bottom sheathing, has a much lower torsional stiffness, and participates less in the reduction of deflection. This unexploited material penalizes the efficiency of the solution (proposal *CP3b_1t* is clearly worse than *CP3a_1t*).

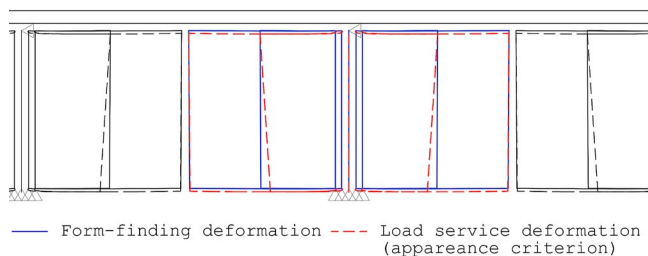


Figure 12. Lateral view of solution *CP3b_1t* elastica: after form-finding process and because of the service load.

Finally, residual stress is also affected by the number of elements and thickness. Actually, the best strategy to reduce the stress due to bending is to reduce plywood thickness. In the case of five-elements joist, *CP3*, bent elements are 9 mm thick. This change in thickness from 12 to 9 mm, together with the movement of the exterior curved element because of the thickness of the intermediate curved panel, manages to reduce form-finding stress of the critical areas (midpoint and ends area) by around 20 % (figure 13).

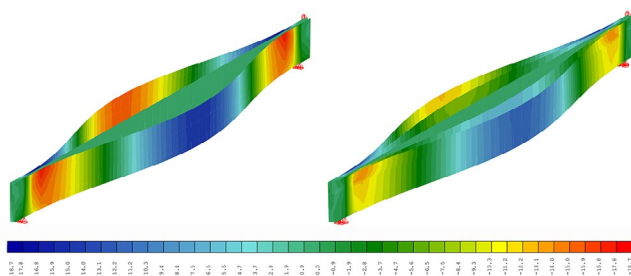


Figure 13. Normal stress for the joist of *CP2a_2t* (left) and *CP3b_2t* (right) after form-finding phase.

3.2. Critical analysis of the computer simulation process

In the field of decision making when designing active bending structures, both the effects on the stiffness of the structure derived from geometry (elastica and camber) and residual stress therein must be considered. Although all these consequences are manifested simultaneously and they are interrelated, the impact of these three results on the stiffness of the

system is unequal, and must be studied in particular: form and camber manage to reduce deformation, while compression prestressing has been revealed as a destabilizing agent.

The cause of the stiffness enhancement for *CP3b_2t* proposal is due to form: the curved pattern arrangement of the nails that connect bottom -and top- sheathing with vertical panels. In order to prevent plug brittle failure in timber nailed connections, Eurocode 5 (18) determines minimum distances between connectors. Depending on the final spacing, the load bearing capacity of the row is no longer that corresponding to the sum of the connectors, and has to be calculated by the effective number of nails. The idea behind the concept of the effective number is the unequal distribution of the load between aligned nails. Compliance with the recommendations of the standard for connector spacing does not alter the mode of stress distribution, as long as the loads are maintained within service values, i.e. if pins do not reach their plastic state, the first and the last ones in the line are more loaded. In Johnsson's experiment, 2004 (19), to test the load distribution in a row of connectors, the most loaded pin is the one closest to the edge. As service load combination for *CP3b_2t* proposal is symmetrical with respect to the central point of the span, then the most loaded nails are those closest to the supports (first and last). Without contravening minimum spacing, to increase the number of intermediate nails in the same line improves the load capacity, but the benefit is qualitatively better if they are divided into new rows of nails. Actually, this is exactly what the curved nail pattern does, which distributes the same number of nails in several rows, of at least 2 nails, along the entire width of the floor (figure 14). This causes that the load transmission to sheathings is substantially greater (the stress at top and bottom sheathing is 50-70 % greater, respectively, according to figure 11).

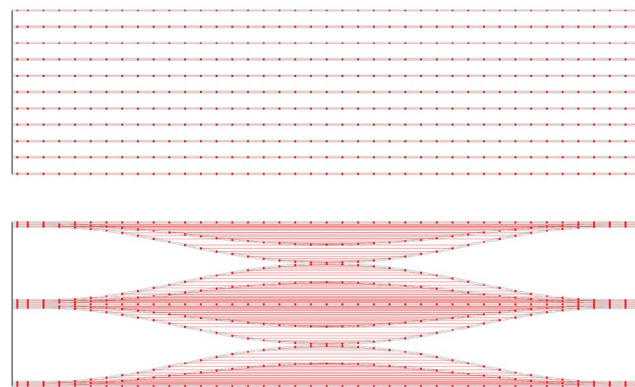


Figure 14. Distribution of nail rows according to grain direction for the grid configuration (top) and the curved nail pattern (bottom). E:1/20. Nails connecting sheathing to joist header are omitted.

The value of camber acts as a subtrahend in the calculation of net final deflection. Therefore, this is a good method to comply with this limitation, which is usually the most restrictive and the one that defines the dimensions of lightweight solutions. In wooden construction, the dimensions that comply with the net final criterion usually comply with the rest of the stiffness criteria -integrity and comfort-, as well as the strength and stability requirements. Therefore, for load hypothesis that generates deformations opposite to those of camber, the benefit is evident: it allows the final deflection to exceed Eurocode 5 net final limitation by a value equal to or less than camber.

3.3. Prototype three-point bending tests

The testing protocol followed includes the breaking of two prototypes in order to isolate the effects of active bending from the benefits derived from the nailing pattern. In this sense, both mockups are built with the same joist scheme. Thus, the first prototype, called *CP2a_1t_c*, has a complete pattern of nails, which join vertical panels to top sheathing. And a second auxiliary prototype, called *CP2a_1t_n*, where only three nails are used to connect the midpoints of the three vertical panels from the joist by means of a small 80 mm wide strip of sheathing (figure 15). Both prototypes are constructed with *lauan* type 1 B-C plywood, M8x100 steel bolts and 1x25 mm nails.

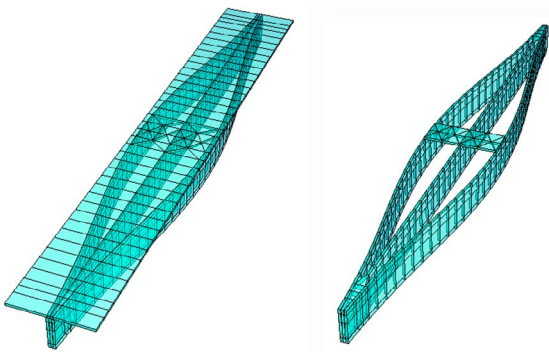


Figure 15. Tested prototypes: *CP2a_1t_c* and *CP2a_1t_n*, left and right.

Both tested mockups (*CP2a_1t_c* and *CP2a_1t_n*) have a non-linear response to the three-point bending test. Both schemes present nonlinearity caused by material yielding, but during the test for the prototype without sheathing (*CP2a_1t_n*), in addition to material nonlinearity, geometric nonlinearity appears. In fact, the main cause of the lack of proportionality between load and deflection is the significant change of the geometry of the prototype during its deformation.

3.3.1. Prototype *CP2a_1t_c*

The behavior of prototype *CP2a_1t_c* during the test agrees with that of the simulation: curved panels twist and the distance between the upper parts of their midpoints remains the same, but the lower parts get closer. At the same time, the straight panel flexes in the direction of loading (figure 16).

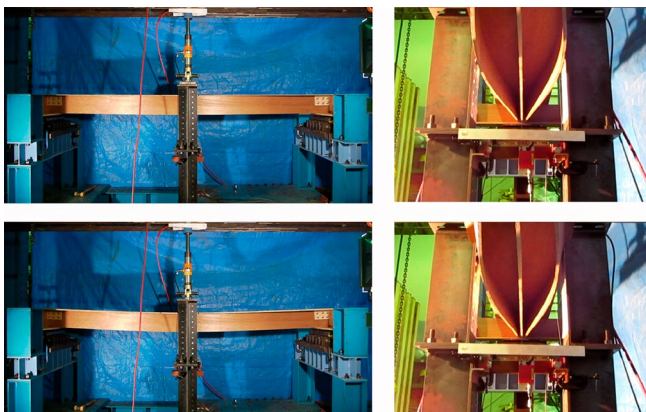


Figure 16. Lateral and bottom view of the three-point bending test of prototype *CP2a_1t_c* when load is 0.5 kN -top- and 4 kN -bottom-.

Figure 17 shows the load-displacement diagram for the three-point bending test of *CP2a_1t_c* prototype. The change in the slope of load-displacement curve seen when applied force is 1.45 kN corresponds to the moment when the upper internal part of bent panels midpoint reaches proportional limit. Due to the plasticization of these zones, the stiffness of the prototype is reduced and the curve shows a lower slope, which is maintained until the structure collapses. This rupture occurs at the midpoint of the straight component when the maximum compressive stress shifts to central panel reaching proportional limit in the upper part, and almost simultaneously, bending strength in the lower zone.

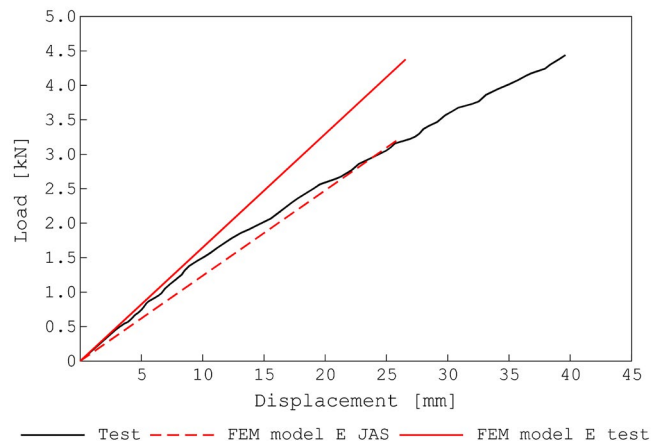


Figure 17. Load-displacement diagram for the three-point bending test of prototype *CP2a_1t_c*.

In addition to test curve, two auxiliary lines are included that reflect FEM analysis of the models when the Young's modulus of material is that corresponding to JAS or that resulted from bending tests carried out specifically on 12 mm *lauan* plywood. It can be seen that the elastic behavior of the prototype coincides with that predicted by the computer model when the value of the elastic modulus used is the result from characterization tests. The line corresponding to the stiffness designated by JAS standard has a less precise adjustment, although it is always on the safe side, and ensures greater deflections than those of the real prototype, even in its plastic phase.

3.3.2. Prototype *CP2a_1t_n*

While in prototype *CP2a_1t_c* the maximum compressive stress was maintained at the top of curved panels (until the moment of rupture when it jumped to the central component), in prototype *CP2a_1t_n* the maximum compressive value was shifting (figure 18).

After joist form-finding, the most stressed areas are bent panels midpoints. During three-point bending test of specimen *CP2a_1t_n*, the zone with the highest compression stress moves, for a force of 1.1 kN, towards the upper external area of curved panels close to the bolts, an area that begins to plasticize for 1.4 kN, since there is no sheathing connecting the upper part of the vertical components. From 2.3 kN onwards the area with the highest stress move to the central panel, until finally the prototype breaks at the bottom of the central plywood.

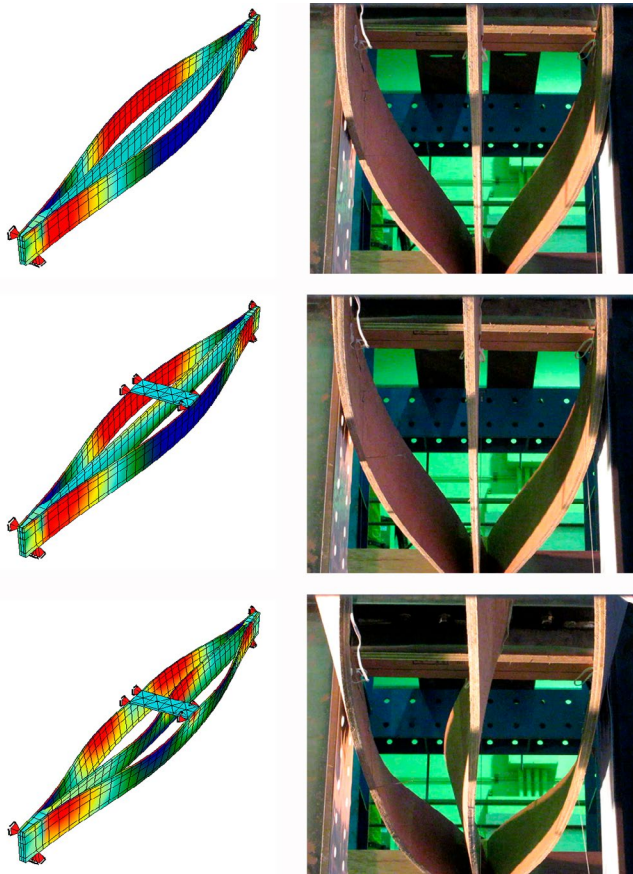


Figure 18. Stress in grain direction and view of the three-point bending test of prototype *CP2a_1t_n* after form-finding process -top-, for a load equal to 1.1 kN -middle- and 2 kN -bottom-.

The failure of prototype *CP2a_1t_n* occurs because bending strength is reached in the middle part of the straight panel (figure 19). The stress at this point depends, during the phase where the prototype behaves elastically, only on the bending caused by the external load. But as soon as the central panel starts to buckle laterally (vertical load equal to 1.4 kN) normal stress increases motivated by straight plywood warping.

Focusing on the benefits derived from active bending, camber and stiffness enhancement due to tensile prestressing, neither of these two effects is measurable in the prototype test, not even in the *CP2a_1t_n* prototype. Deflection caused by self-weight (0.55 mm) already neutralizes the camber originated during form-finding process (-0.14 mm). Moreover, tensile prestress of the central panels is cancelled when the point load reaches 0.14 kN, and the onset of loading process of prototype arrives at 0.47 kN. So load-deflection curve of the tests does not present any change of slope caused by active bending.

3.4. Critical analysis of three-point bending tests

Figure 20 shows the load-displacement curves of the three-point bending test of both the specimens *CP2a_1t_c* and *CP2a_1t_n*. If the elastic sections of both curves are compared, it is observed that both solutions start to plasticize for approximately the same load. In the nailed solution, the curved panels midpoint starts to plasticize for a point load equal to 1.45 kN. And in the non-nailed option, it is the area near the bolts that plasticizes for a load of 1.4 kN.

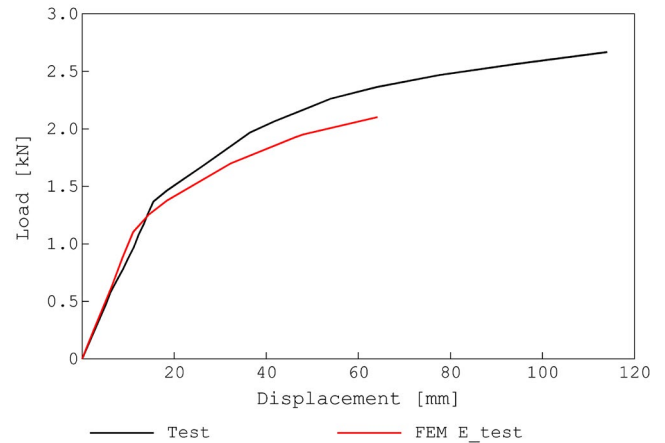


Figure 19. Load-displacement diagram for the three-point bending test of prototype *CP2a_1t_n*.

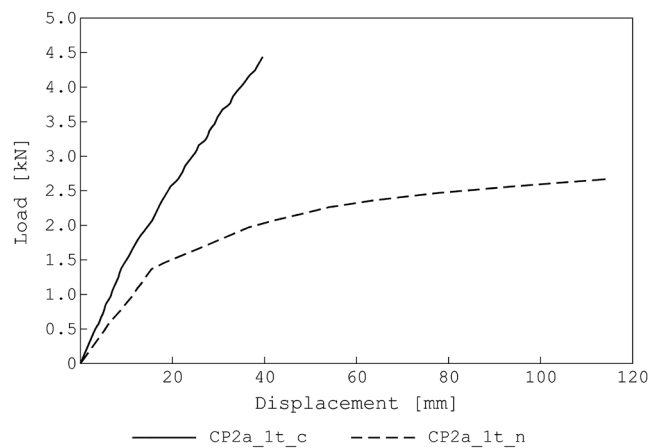


Figure 20. Comparative load-displacement diagram of the three-point bending test of prototype *CP2a_1t_c* and *CP2a_1t_n*.

This concurrence occurs because the residual stress of both zones is very close to the proportional limit resulted from bending experiments for 12 mm JAS Class 1 B-C *lauan* plywood: the area near the bolts of curved panels reaches 84 % while midpoint reaches 92 % of proportional limit. Although this adjustment may seem excessive, the reason why it was chosen to approach so close to the elastic limit is because of the distance still existing with respect to failure strength: 64 % and 71 % of the value resulted experimentally. Nevertheless, and even that when loaded uniformly the elastic limit is reached for a higher load, 2.8 kN/m², it seems logical to aspire to extend the length of the elastic behavior. In this sense, the conclusions emerged from this thought ended up improving the design of more efficient proposals (group CP3).

If nonlinear sections are included in the comparison, *CP2a_1t_n* prototype is less strong, and much less stiff. The ultimate deflection for non-nailed scheme is 2.85 times higher than the nailed model. This difference is based on the fact that the nonlinearity of the model *CP2a_1t_c* is purely material, while the prototype *CP2a_1t_n* has, in addition to the one produced by the material, geometric nonlinearity. So the first purpose of nails is that they prevent lateral buckling of straight panel. This is also demonstrated by the fact that, although the central component of *CP2a_1t_n* prototype was

laterally constraint only by a single 1 mm diameter nail located at midpoint, this is enough to modify the buckling form. Thus, due to the effect of the intermediate nail, elastica of central plywood of the experiment is the sinusoid of two arcs, instead of the simpler elastica of a single arc.

Once tested, both specimens were disassembled for the classification of their components and recycling. Firstly, sheathing of prototype *CP2a_1t_c* was removed, which allowed to check the condition of the nails and none of them had broken or become plasticized (figure 21). In spite of the fact that the diameter of the nails chosen for the joint between sheathing and vertical panels, equal to 1 mm, is less than that established in the UNE-EN 14592 standard, which sets the minimum nominal diameter at 1.9 mm, it is shown that their mechanical behavior is sufficient enough for this application.



Figure 21. Photograph of the condition of sheathing nails after the three-point bending test of prototype *CP2a_1t_c*.

4. CONCLUSIONS

The effects of active bending on several floor structure proposals made from plywood are evaluated. Since bent form only depends on the length ratio of the elements, floor slabs can be easily mass prefabricated by a robot supported manufacturer and then be transported to construction site. During the structure erection, all building tasks will benefit from the slab lightness.

Concerning analytical study, the concepts of structural consumption quantification devised by Frei Otto's working

group were applied. This appraisal has shown that the proposal identified as *CP3b_2t* -with five elements per joist and top and bottom sheathing- has a mass 11 % lower than the straight and parallel joists system that achieves the same deformation for identical load.

Camber and prestress may improve the performance of the system, but the main cause of stiffness enhancement for *CP3b_2t* proposal is due to form. The curved pattern arrangement of the nails connecting vertical panels to sheathing is stiffer than the grid pattern from straight joists solutions: increasing the number of intermediate nails in the same line improves load capacity, but the benefit is qualitatively better if new rows of nails are introduced.

The main conclusions derived from the three-point bending test of the tested in-plane bending prototypes are three: non-linear behavior of the tested proposal starts at a relatively low load, any benefit derived from camber or prestress has been almost irrelevant, and the usefulness of experimental tests as a tool to find out instabilities that otherwise would be difficult to predict only by computational means. However, although these conclusions are described here, they have to be understood as conclusions that correspond to an intermediate work process, as they were used to feed back the development of the analytical part.

From the comparison of the tests for full scale prototypes *CP2a_1t_c* and *CP2a_1t_n*, a clear lesson was drawn: form-finding stress should have to be lowered to achieve a proposal with the same form but with a greater elastic span. Or at least, stress caused by service loads in the areas where maximum values are reached should increase more slowly. Strategies that achieve these objectives involve reducing the thickness of bent panels and/or increasing the number of curved elements in the joist. In order to implement these solutions, the number of cases to be analyzed computationally was increased by incorporating the proposals designated as *CP3* -with four bent panels-. Actually, one of the new added schemes is the one that would end up being the most efficient (*CP3b_2t*).

5. ACKNOWLEDGEMENTS

This research has been partially supported by the Erasmus Mundus EASED programme (Grant 2012-5538/004-001) coordinated by CentraleSupélec.

REFERENCIAS / REFERENCES

- (1) Lienhard, J.; Schleicher, S.; Knippers, J. (2011). Bending-active Structures – Research Pavilion ICD/ITKE. *Taller, longer, lighter*. Proceedings of the International Symposium of the IABSE-AISS Symposium, London, UK, 2011. London: Nethercot, D., Pellegrino, S. et al. (eds).
- (2) Lienhard, J.; Alpermann, H.; Gengnagel, C.; Knippers, J. (2012). Active bending, a review on structures where bending is used as a self-formation process. *International Journal of Space Structures*, 28, 187-196. <https://doi.org/10.1260/0266-3511.28.3-4.187>
- (3) Ochsenschlager, E. (1998). Life on the edge of the marshes. *Expedition* 40 (2): 29-40. Philadelphia: University of Pennsylvania, Museum of Archaeology and Anthropology.
- (4) Émy, A.R. (1837). *Traité de l'art de la Charpenterie*. Anselin libraire. Paris, France.
- (5) Happold, E. and Liddell, I. (1975). Timber lattice roof for Mannheim Bundesgartenschau. *The Structural Engineer*, 3, Volume March 1975, 99-135.
- (6) Otto, F. et al. (1998). *IL 24 – Lightweight principle*. Stuttgart: Institute for Lightweight Structures. Germany.
- (7) Schaur, E. (1979). *IL 21 – Basics: Form-Force-Mass*. Stuttgart: Institute for Lightweight Structures. Germany.
- (8) Otto, F. (1985). *Konzepte SFB 230*. Stuttgart: Institute for Lightweight Structures. Germany

- (9) Kull, U.; Herbig, A.; Otto, F. (1992). Construction and Economy of Plant Stems as Revealed by Use of the Bic-method. *Annals of Botany* 69, 327,334. University of Oxford. England.
- (10) Otto, F. (1968). *Biotechnik-7. Natur und Leichtbau, Vergleich der Konstruktion*. DIA Ausstellungstafeln, Berlin. Germany.
- (11) García Santabárbara, A., Cervera Bravo, J. (2017). Conceptos para la cuantificación del consumo estructural y su aplicación a estructuras generadas por elementos prelectados. *Informes de la Construcción*, 69(546), e201. <http://doi.org/10.3989/ic.16.016> (in spanish).
- (12) Gengnagel, C.; Alpermann, H.; Lafuente, E. (2014). Active Bending in Hybrid Structures. *FORM – RULE | RULE – FORM 2013*. Innsbruck University Press. Germany.
- (13) Lienhard, J. (2014). *Bending-Active Structures. Form-finding strategies using elastic deformation in static and kinetic systems and the structural potentials therein*. (doctoral thesis). Universität Stuttgart, Germany.
- (14) Forest Product Laboratory (1999). Wood handbook – Wood as an engineering material. F.P.L. Madison, Wisconsin.
- (15) Paradis et al. (2015). *Tropix 7* (consulted version 7.5.1.) CIRAD. France.
- (16) JAS (Japanese Agricultural Standard). *Structural plywood standard*. Japan's Ministry of Agriculture, Forestry and Fisheries
- (17) Bathe, K. (1996). *Finite Element Procedures*. Prentice Hall. New Jersey, USA.
- (18) EN 1995-1-1:2004. *Eurocode 5: Design of timber structures - Part 1-1: General - Common rules and rules for buildings*.
- (19) Johnsson, H. (2004). *Plug shear failure in nailed timber connection. Avoiding brittle and promoting ductile failures* (doctoral thesis). Luleå University of Technology. Luleå, Sweden.